# Specification Method of Surface Measurement for Surgical Navigation: Ridgeline Based Organ Registration

Naomichi Furushiro[1], Tomoharu Saito[2], Yoshitaka Masutani[3], and Ichiro Sakuma[2]

[1] Department of Precision Engineering, Graduate School of Engineering,
the University of Tokyo, Hongo 7 3 1, 1138656 Tokyo Bunkyo, Japan
naof@intellect.pe.u-tokyo.ac.jp
[2] Institute of Environmental Studies, Graduate School of Frontier Sciences,
the University of Tokyo, Hongo 7 3 1, 1130033 Tokyo Bunkyo, Japan
{tomoharu,sakuma}@miki.pe.u-tokyo.ac.jp
[3] Department of Radiology, Faculty of Medicine,
the University of Tokyo, Hongo 7 3 1, 1130033 Tokyo Bunkyo, Japan
masutani@cim.pe.u-tokyo.ac.jp

**Abstract.** Surgical navigation for abdominal organs has difficulties, such as dynamic deformation, compared with other organs (i.e. brain, bone). Organ deformations prevent surgical navigators from performing accurate navigation based on preoperative information. We are studying on a method for deforming preoperative organ models so that the models are matched to intraoperative shapes. The method is based on the ICP (iterative closest point) algorithm and modal representation of shape deformation. In this paper, we describe preliminary experiments for rigid parameter estimation in the entire registration process, by using range data and surface model reconstructed from X-ray CT of a liver phantom.

## 1 Introduction

One of the difficulties in surgical navigation based on preoperative image information is intraoperative deformation of the organs consisting of soft tissues. In neurosurgery, for instance, “brain-shift” is recognized as an essential reason of navigation errors. A simulation of brain deformation was reported by Ferrant [1], based on the finite element method (FEM) for reduction of errors in neurosurgical navigation. In hepatic surgery, however, the shape of liver deforms more dynamically due to patient respirations, posture changes, and surgical operations. Those intraoperative liver deformation includes so-called large displacement, and therefore it requires much more computation cost for numerical simulation based on non-linear FEM. Cotin [2] and Picinbono [3] reported development of a surgical simulator based on fast computation technique of non-linear FEM to show realistic liver deformation of large displacement. For our purpose of surgical navigation, however, relationship between force and displacement is not important, but deformation of preoperative models for registration to intraoperative shape is indispensable for surgical guidance. Herline [4] reported rigid liver surface registration for such purpose. In that literature, many methods for deformation description can be found, including parametric description for non-rigid tracking of objects, and for animation [5-8]. In such parametric descrip-

T. Dohi and R. Kikinis (Eds.): MICCAI 2002, LNCS 2489, pp. 109–115, 2002.

tions, generally, shape deformation should be represented with fewer parameters for faster operation. Masutani [9] reported a new method of modal representation of liver deformation applied for intra-operative non-rigid registration in image-guided liver surgery. In that literature, several experiments with synthetic range data were performed based on error factor analyses. In this paper, we present detailed a new method of rigid-body registration using ridgelines extracted from range images.

## 2 Materials and Methods

### 2.1 Liver Phantom and Its Reconstructed 3-D Model

We made a full-scale model of a liver with silicone rubber. Fig. 1. shows the liver phantom model. The size of the phantom is about 210 mm × 180 mm, and the thickness is about 100 mm to 200 mm. We took a series of X-ray CT scan of the phantom and reconstructed the data. Fig. 2. shows the reconstructed 3-D model of the liver phantom.

**Fig. 1.** A silicone rubber phantom model of a liver. The shape of the liver was segmented from a series of abdominal X-ray CT images

**Fig. 2.** 3-D reconstructed model of the liver phantom shown in Fig. 1. Shape data of the phantom was acquired by X-ray CT scanning in 0.9 mm thick

### 2.2 Range Images and Surface Data Acquisition

We use a range sensor based on space encoding method. The sensor has 0.5 mm accuracy, and its view area is about 200 mm × 200 mm at 300 mm away from the sensor. We can take a picture and a range image of a view with the same optical axis in one second. Fig. 3. shows a range image of the liver phantom model, and Fig. 4. shows its photo image. The resolutions of the sensor are 512 × 240 pixels at view plane, and 8 bit (256 scale) in depth direction. We also obtain 3-D coordinate values at each point of a view plane. The origin point of the coordinate system is 300 mm Away from the sensor in depth direction. Gray values of a range image represent the depth at each point; the origin plane is black, and the nearer a point, the brighter the color of the point become.

### 2.3 Ridgeline Extraction from Range Images

Fig. 5. shows the conceptual diagram of our system . Ridgeline extraction is as follows.

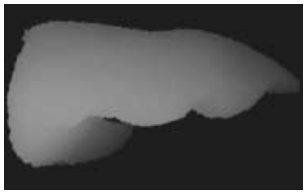

**Fig. 3.** A range image of the phantom obtained with range sensor from the distance of 220 mm

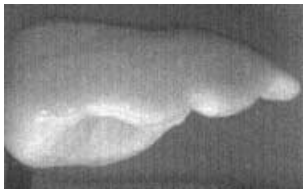

**Fig. 4.** A photo image of the phantom taken at the same time with a range image (Fig. 3)

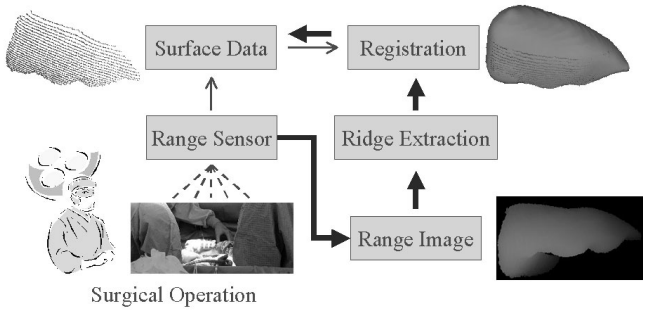


**Fig. 5.** Conceptual diagram of the system

**Preparation of Range Images**

We apply a normal distribution gauss function filter to range images to reduce noises and smooth the images (1).

$$g(x, y; t) = \frac{1}{2\pi t} \exp\left(-\frac{x^2 + y^2}{2t}\right) \tag{1}$$

where $t$ represents the radius of the gauss function filter.

**Curvature Computation**

We compute curvatures of each point using its gray values after gaussian filter. Here we define $L_x$ as the first differential value of gray value $L$, and also define $L_y$, $L_{xx}$, $L_{xy}$, and $L_{yy}$ in the same manner, then we can compute the principal curvatures (2).

$$\kappa_1 = \frac{-(L_{xx} - L_{yy}) + \sqrt{(L_{xx} - L_{yy})^2 + 4L_{xy}^2}}{2\sqrt{1 + L_x^2 + L_y^2}}$$

$$\kappa_2 = \frac{-(L_{xx} - L_{yy}) - \sqrt{(L_{xx} - L_{yy})^2 + 4L_{xy}^2}}{2\sqrt{1 + L_x^2 + L_y^2}} \tag{2}$$

**Classification of Shapes**

We can classify the shape of each point using the principal curvatures. The classification is carried out along the shape index *S*, which represents the ratio of principal curvatures and its value is between zero and one (3). Table 1. shows how shapes change according to the value of *S*.

$$S = \frac{1}{2} + \frac{1}{\pi} \tan^{-1} \frac{\kappa_1 + \kappa_2}{\kappa_1 - \kappa_2} \tag{3}$$

**Table 1.** The Classification of Shapes with the value of *S*

| *S* | Shape type |
|---|---|
| 0 to 0.125 | Pit |
| 0.125 to 0.375 | Valley |
| 0.375 to 0.625 | Saddle |
| 0.625 to 0.875 | Ridge |
| 0.875 to 1 | Peak |

We also compute the curvedness *R*, which represents the magnitude of the curvature at each point (4).

$$R = \frac{\sqrt{\kappa_1^2 + \kappa_2^2}}{2} \tag{4}$$

**Ridgeline Extraction**

We extract ridge area weighting curvedness *R* with the shape index *S* (5).

$$R' = R \times \exp\left(-\frac{(0.75 - S)^2}{\sigma_r}\right) \tag{5}$$

Fig. 6. shows the area for weighting *R*.

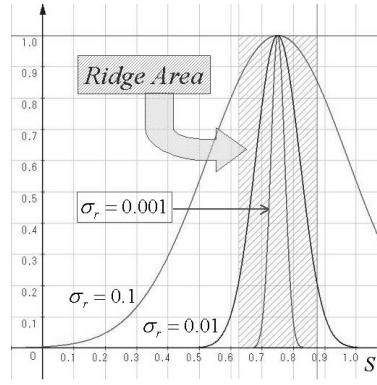


**Fig. 6.** Weighting factor for the curvedness R along with the shape index S

### 2.4 Registration Method

We use a curve matching method with ICP (Iterative Closest Point) algorithm to register these extracted ridgelines. Before registering measured surface data with model data, we compute ridgeline of the model. Fig. 7. shows the ridgelines of 3-D reconstructed model. After the ridgeline registration, we register measured surface point data to the surface points of model data with ICP algorithm.

**Fig. 7.** Ridge areas of 3-D reconstructed model of the phantom

## 3 Results

### 3.1 Ridgeline Extraction from Range Images

We extract a ridgeline from the range image shown at Fig. 3. The ridgeline locates at the front side of the liver phantom model. The parameters to extract this are gaussian filter radius, weighting area limitation. We use 7 as gaussian filter radius for equation (1), and 0.01 as weighting area limitation number for equation (5). Fig. 8. shows the result of extracted ridgeline image.

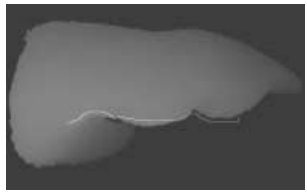

**Fig. 8.** A ridgeline extracted from the range image of Fig. 3

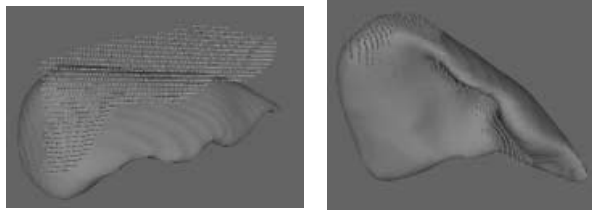

(a) (b)

**Fig. 9.** Result of ridgeline registration. (a)Before registration, (b)After registration

### 3.2 Ridgeline Registration Result

Before the ridgeline registration, RMS error between the measured surface point data and the surface data of model was 36.83 mm. After the ridgeline registration, RMS error became 10.24 mm. Fig. 9. shows the locations of measured data and the model data.

### 3.3 Point Based Registration

After the ridgeline registration, we apply measured point data to ICP algorithm to register these data to the surface of the model. The number of measured points was 1528, and that of the model was 5479. The algorithm converged at 11th iteration, and the final RMS error was 1.68 mm. Fig. 10. shows the final location of measured surface and the model.

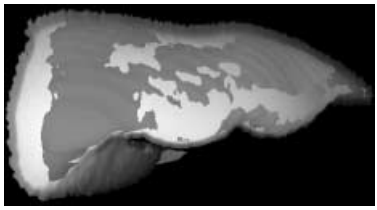

**Fig. 10.** Registered range data of the phantom with 3-D reconstructed model of the phantom

## 4 Discussion

One of the most important properties of our method is that our system is independent to particular points of organs. To achieve the registration, we prepare ridgeline based posture estimation. This method is not only for the use of celiotomies, but also endoscopic surgery. Our purposes of surgical navigation system development include guidance of surgical robots. One of the potential advantages of such robotic surgery is that surgical operations can be carried out with minimal deformation of organs. Therefore, robotic surgery with navigational information based on our registration method is expected to realize more precise and minimally invasive surgeries.

## 5 Summary

For intra-operative rigid registration in image -guided liver surgery, a new method for surface measurement based registration was proposed. By using a liver phantom model, the registration error for frontal displacement was aligned. Toward feasibility study in clinical environment, studies using deformed phantom, and collection of intraoperative data are currently in progress.

## Acknowledgements

This work is a part of the research project: *development of robotic surgery system* in *Research for the Future Program* of Japan Society for Promotion of Science (JSPS) and is financially supported by JSPS. The authors are grateful to Dr. Makoto Hashidume for clinical advice, and to all the project members for the inspiring discussion, and to Dr. Shigeru Nawano in the eastern hospital of National Institute of Cancer Center – Japan, for providing the patient CT data set used in this study.

## References

1. M. Ferrant, et al. Registration of 3D Intraoperative MR Images of the Brain Using a Finite Element Biomechanical Model proc. of MICCAI2000 pp.19-27 2000
2. S. Cotin, et al. Real-Time Elastic Deformations of Soft Tissues for Surgery Simulation IEEE trans on Visualization and CG vol.5 no.1 pp62-73 1999
3. G. Picinbono, et al. Non-Linear Anisotropic Elasticity for Real-Time Surgery Simulation INRIA tech. rep. No4028 2000
4. J. Herline, et al. Surface Registration for Use in Interactive Image –Guided Liver Surgery proc. of MICCAI99 1999
5. D. Terzopoulos,et al. Dynamic 3D Models with Local and Global Deformations: Deformable Superquadradrics IEEE trans on PAMI vol.13 no.7 pp703-714 1991
6. S. Sclaroff, et al. Modal Matching for Correspondence and Recognition Boston U. tech. rep. TR95-008, 1996
7. G. Szekely, et al. Segmentation of 2-D and 3-D objects from MRI volume data using constrained elastic deformations of flexible Fourier contour and surface models Medical Image Analysis vol.1 no.1 pp19-34, 1996
8. G. C. H. Chuang, et al.Wavelet Descriptor of Planar Curves: Theory and Applications IEEE trans on Image Proc. vol.5 no.1pp.56-70 1996
9. Y. Masutani and F. Kimura A New Modal Representation of Liver Deformation for Non-Rigid Registration in Image-Guided Surgery, proc. Of CARS2001 pp.19-24 2001